



OPEN

Altered cardiac mitochondrial dynamics and biogenesis in rat after short-term cocaine administration

Shuheng Wen, Kana Unuma, Takeshi Funakoshi, Toshihiko Aki[✉] & Koichi Uemura

Abuse of the potent psychostimulant cocaine is widely established to have cardiovascular consequences. The cardiotoxicity of cocaine is mainly associated with oxidative stress and mitochondrial dysfunction. Mitochondrial dynamics and biogenesis, as well as the mitochondrial unfolded protein response (UPR^{mt}), guarantee cardiac mitochondrial homeostasis. Collectively, these mechanisms act to protect against stress, injury, and the detrimental effects of chemicals on mitochondria. In this study, we examined the effects of cocaine on cardiac mitochondrial dynamics, biogenesis, and UPR^{mt} in vivo. Rats administered cocaine via the tail vein at a dose of 20 mg/kg/day for 7 days showed no structural changes in the myocardium, but electron microscopy revealed a significant increase in the number of cardiac mitochondria. Correspondingly, the expressions of the mitochondrial fission gene and mitochondrial biogenesis were increased after cocaine administration. Significant increase in the expression and nuclear translocation of activating transcription factor 5, the major active regulator of UPR^{mt}, were observed after cocaine administration. Accordingly, our findings show that before any structural changes are observable in the myocardium, cocaine alters mitochondrial dynamics, elevates mitochondrial biogenesis, and induces the activation of UPR^{mt}. These alterations might reflect cardiac mitochondrial compensation to protect against the cardiotoxicity of cocaine.

Cocaine (benzoylmethylecgonine), a strongly addictive psychostimulant, is the second most commonly used recreational drug in the world¹. Sufficient evidence shows that the use of cocaine is related to a series of dangerous cardiovascular consequences, such as coronary artery spasm², dysrhythmia^{3,4}, hypertension⁵, left ventricular hypertrophy⁶, and myocardial infarction^{7,8}. In addition to the anesthetic effect of cocaine by blocking sodium channels, the cocaine-induced cardiovascular disorders are mainly due to its potent sympathomimetic effect, which is achieved by the blockage of catecholamine reuptake at neuronal presynaptic terminals^{9,10}. This allows cocaine not only to escalate the myocardial oxygen demand, but also, simultaneously, to decrease the myocardial oxygen flow^{11,12}. In general, oxidative stress and mitochondrial dysfunction in cardiomyocytes are believed to play pivotal roles in cocaine-induced cardiotoxicity^{13–17}.

Cardiac mitochondria, which occupy 20–40% of the cardiac cellular volume, are indispensable for producing the copious amounts of ATP required to sustain the unremitting contraction of the myocardium^{18–20}. Moreover, mitochondria are implicated in the maintenance of intracellular Ca²⁺ homeostasis, the regulation of cell death and survival, and are the primary origin of the reactive oxygen species (ROS) that trigger oxidative stress when overproduced^{21–23}. Studies have found that mitochondria play a key role in cardiovascular pathogenesis, such as dysrhythmia and heart failure^{24,25}. Thence, the homeostasis and normal function of mitochondria are crucial for the ideal operation of the heart, and these are sustained by mitochondrial dynamics and biogenesis²⁶.

Mitochondrial dynamics, which refers to the continuous fusion-fission circulation of mitochondria, is regulated by a series of dynamin-related GTPases^{27,28}. Briefly, optic atrophy 1 (OPA1) and mitofusin (MFN) 1 and 2 facilitate mitochondrial fusion^{27,29}. On the other hand, dynamin-related protein 1 (Drp1), which plays a leading role in mitochondrial fission, is phosphorylated and recruited to the fission point. Phospho-Drp1 (p-Drp1) then promotes the formation of a membrane constriction ring by reactions with receptors and Drp1 oligomerization, which then leads to the completion of mitochondrial fission^{28,30,31}. Mitochondrial biogenesis, on the other hand, is driven by peroxisome proliferator-activated receptor (PPAR) γ coactivator 1 α (PGC-1 α)³². Effectors of PGC-1 α ,

Department of Forensic Medicine, Graduate School of Medical and Dental Sciences, Tokyo Medical and Dental University (TMDU), 1-5-45 Yushima, Bunkyo-ku, Tokyo 113-8519, Japan. ✉email: aki.legm@tmd.ac.jp

such as PPAR α , as well as transcription factors such as nuclear respiratory factor 1 (NRF1) and mitochondrial transcription factor A (TFAM) also participate in the regulation of mitochondrial biogenesis³³. Mitochondrial dynamics and biogenesis form a delicate coping mechanism to maintain the optimal energetic output of mitochondria in response to different environments, including increased oxidative stress and toxic conditions^{27,28,34,35}. They are closely associated with the homeostasis of the cardiovascular system and an altered balance of mitochondrial dynamics can lead to pathological cardiac remodeling and cardiac pathogenesis^{19,36–38}. Accordingly, the status of mitochondrial dynamics and biogenesis is fascinating when against the cardiotoxicity of cocaine. Recently, the protective role of the mitochondrial unfolded protein response (UPR^{mt}) in cardiac pathophysiology has drawn increasing attention. During the accumulation of mitochondrial stress, activated UPR^{mt} promotes the recovery of the oxidative phosphorylation machinery³⁹, restores proteostasis⁴⁰, and detoxifies excess ROS⁴¹, accomplished by the translocation of its major regulator, activating transcription factor 5 (ATF5), and the activation of mitochondrial resident chaperones and proteases^{42,43}. It remains unrevealed whether UPR^{mt} participates in resistance to the cardiotoxicity of cocaine.

Here, we investigate whether cocaine affects cardiac mitochondrial dynamics and biogenesis *in vivo*. After rats were administered 20 mg/kg/day cocaine via the tail vein for 7 days, we found strengthened cardiac mitochondrial fission and biogenesis, as well as the recruitment of PPAR α , while the expressions of mitochondrial fusion factors were decreased. In addition, UPR^{mt} was shown to be activated, although only a panel of its downstream effector gene expressions were indeed upregulated. We believe that this is the first *in vivo* study showing the altered mitochondrial dynamics and biogenesis, as well as the involvement of PPAR α and UPR^{mt}, in cardiomyocytes after cocaine administration.

Materials and methods

All methods were carried out in accordance with relevant guidelines and regulations.

Animals and cocaine administration. All animal experiments were approved by the Institutional Animal Care and Use Committee of Tokyo Medical and Dental University. All animal work was performed in accordance with Animal Research: Reporting of In Vivo Experiments (ARRIVE) guidelines and regulations. Male Sprague Dawley rats (8 weeks old) were randomly divided into 3 groups ($n = 4$, respectively) and administered saline (control group) or cocaine [low (5 mg/kg)/ high (20 mg/kg) dose cocaine group] in the first-round experiments. In second-round experiments to further examine expressions of oxidative phosphorylation system proteins, complex I activity, the protein expressions of UPR^{mt} factors and PPAR α , and to obtain samples for transmission electron microscopy, a control group ($n = 4$) and a high dose cocaine group ($n = 7$) were established under the same condition as the first-round experiments. Findings of the two rounds of experiments are shown collectively to provide a comprehensive demonstration of the consequences of cocaine cardiotoxicity.

Dose conversions from humans to rats were made to establish the conditions of 5 and 20 mg/kg/day to represent typical serum concentrations for recreational cocaine abusers and beneath the concentrations for acute cocaine poisoning overdose^{44,45}. Cocaine hydrochloride (Shionogi & Co., Ltd., Osaka, Japan) was dissolved in saline and administered intravenously via the tail vein (5 mg/kg/day for the low dose cocaine group, 20 mg/kg/day for the high dose cocaine group) for 7 days. Control rats received the same volume of saline injected via the tail vein on the same schedule. The rats were sacrificed by an overdose of sodium pentobarbital (40 mg/kg, intraperitoneally) 24 h after the last administration. The hearts were immediately harvested and placed in phosphate-buffered saline solution (PBS, 4 °C, pH 7.4). Subsequently, the left ventricles were evenly divided for further histological and biochemical analyses.

Histological analysis and immunohistochemical staining. The left ventricular specimens for microscopy were fixed in 4% paraformaldehyde, embedded in paraffin, and 2.5 μm -thick sections were prepared. Hematoxylin–eosin (H&E) and Elastica-Masson-Goldner (EMG) staining were performed for histological analysis. Immunohistochemical staining of PPAR α and ATF5 were conducted. Briefly, sections were deparaffinized in xylene, rehydrated with a series of graded ethanol, and heated in 10 mM citrate buffer (pH 6.0) for antigen retrieval. 3% hydrogen peroxide was applied afterward to quench the activity of endogenous peroxidase. The sections were then blocked with 0.5% bovine serum albumin serum in PBS. Subsequently, the sections were incubated with rabbit anti-ATF5 monoclonal antibody (diluted 100-fold; ab184923, Abcam, Cambridge, UK) or mouse anti-PPAR α monoclonal antibody (diluted 100-fold; sc-398394, Santa Cruz Biotechnology, Inc., USA) overnight at 4 °C, followed by visualization of antigens by use of Histofine simple stain MAX-PO (Multi) (Nichirei Biosciences Inc., Tokyo, Japan) using diaminobenzidine (Nichirei Biosciences Inc.) as a substrate. Sections incubated in PBS in place of the primary antibodies were used as controls for immunostaining procedures.

Mitochondrial electron transport chain activity detection. The left ventricle specimens for mitochondrial complex I enzyme activity analysis were immediately frozen to -80 °C. Mitochondria were extracted from the specimens using a Mitochondria Isolation Kit (ab 110168, Abcam). The protein concentrations of the extracts were determined by Bicinchoninic Acid protein assay and adjusted to 100 $\mu\text{g}/\text{mL}$ with PBS. Subsequently, a Complex I Enzyme Activity Assay Kit (ab109721, Abcam) was used to determine the activity of the electron transport chain (ETC) following the manufacturer's protocol. The absorbance at 450 nm was measured using a microplate reader (GloMax Discover System GM3000, Promega Corporation, USA).

Immunoblotting analysis. The left ventricle specimens for immunoblotting were lysed in STE buffer (320 mM sucrose, 10 mM Tris–HCl, 5 mM EDTA, 50 mM NaF, 2 mM Na₃VO₄, and protease inhibitor cocktail (Roche Diagnostics, Mannheim, Germany)), and the lysates were subjected to SDS–polyacrylamide gel elec-

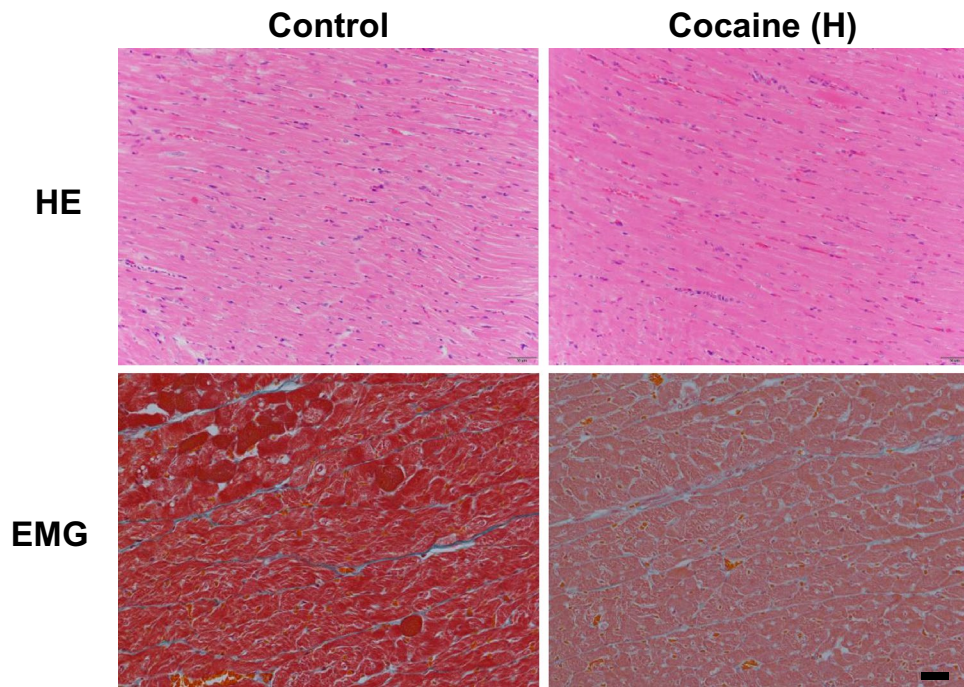


Figure 1. Microscopy of myocardium after cocaine administration. Hematoxylin and Eosin (HE) and Elastica-Masson–Goldner (EMG) staining of rat left ventricular samples from control and cocaine high dose groups, cocaine (H), cocaine high dose group, scale bar = 50 μ m.

trophoresis. Immunoblotting was then performed with voltage-dependent anion channel 2 (VDAC2) antibody (#9412, Cell Signaling Technology, Beverly, MA, USA), the translocase of the outer mitochondrial membrane 20 (TOM20) antibody, (#42406, Cell Signaling Technology), total OXPHOS Rodent WB antibody cocktail (ab110413, Abcam), anti-PGC-1 polyclonal antibody (#AB3242, EMD Millipore Corporation, CA, USA), anti-NRF1 antibody (sc-33771, Santa Cruz Biotechnology, Inc.), anti-TFAM antibody (sc-23588, Santa Cruz Biotechnology, Inc.), anti-PPAR α monoclonal antibody (Santa Cruz Biotechnology, Inc.), anti-ATF5 rabbit monoclonal antibody (Abcam), anti-CHOP mouse monoclonal antibody (#2895, Cell Signaling Technology), and anti-actin antibody (A2066, Sigma-Aldrich, St. Louis, MO, USA). Antigens were visualized by peroxidase-bonded anti-Mouse or rabbit IgG secondary antibodies (Promega Corporation, USA) and enhanced chemiluminescence reagents (Thermo Fisher Scientific, USA). The band densities were quantified by CS analyzer 4 image analyzing software (Atto, Tokyo, Japan).

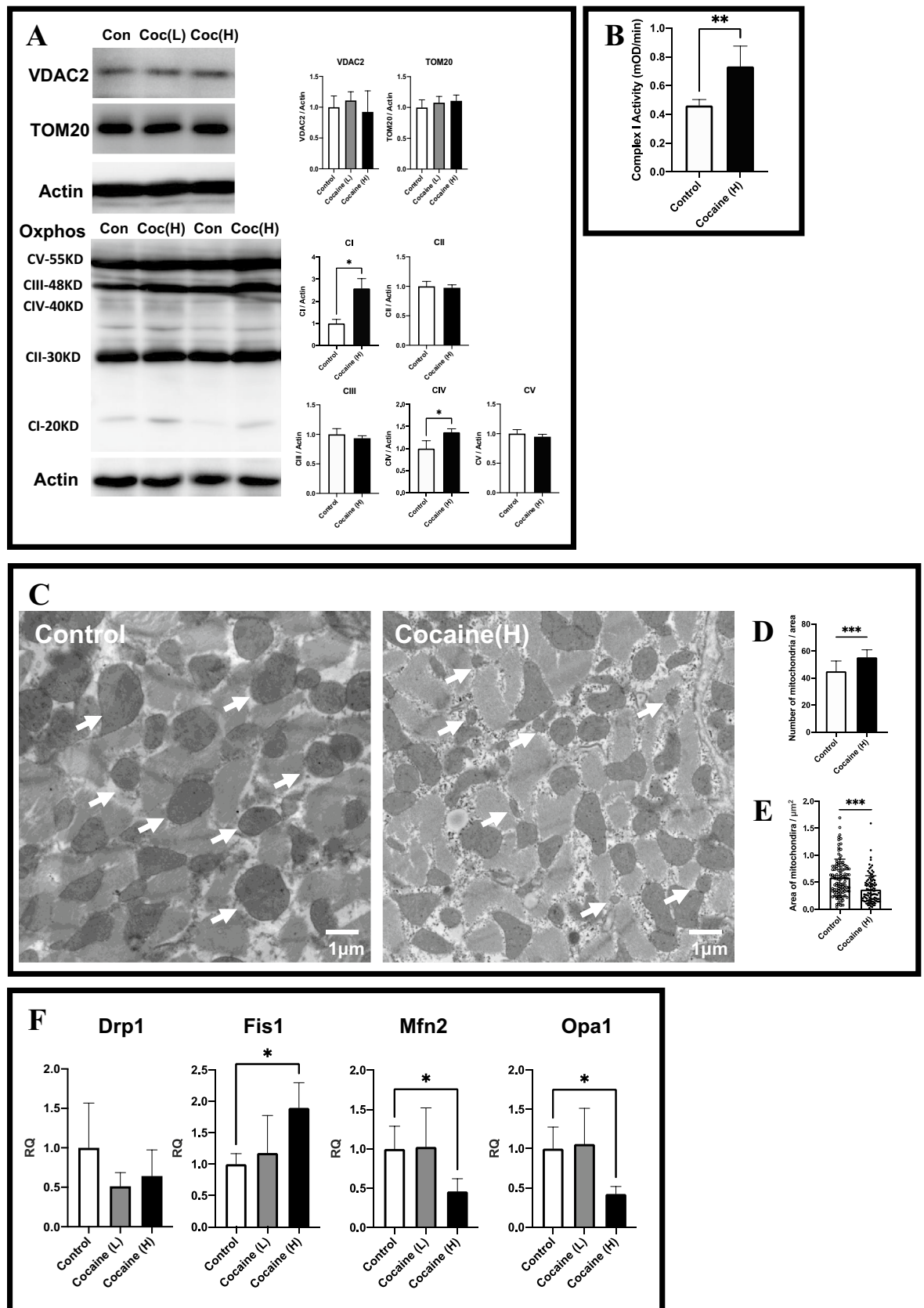
Transmission electron microscopy. The left ventricle specimens for electron microscopy were washed with 0.1 M phosphate buffer (PB) and fixed with 4.5% paraformaldehyde and 2.5% glutaraldehyde in PB. After incubated in 1% osmium tetroxide for 2 h, the fixed specimens were dehydrated in a series of graded ethanol and embedded in Epon epoxy resin. Ultrathin sections of the embedded specimens were stained with uranyl acetate and lead citrate and observed under a transmission electron microscope (H7100, Hitachi, Japan) and AMT Advantage-HS CCD camera (AMT, Woburn, USA). The number of mitochondria per field (magnitude: 10,000 \times) was counted from 10 electron micrographs in each group. Randomly selected cross-sectional areas of mitochondria ($n = 100$ for each group) in cross-sectional views of cardiac myofibrils were counted using ImageJ software (ver1.53).

Real-time reverse transcriptase-mediated PCR analysis. Real-time reverse transcriptase-mediated PCR analysis was conducted as described previously⁴⁶. The primers used are listed in Supplementary Table S1.

Statistical analysis. Student's t-test and Dunnett's test were used to assess statistical significance throughout this study. Statistical differences were considered significant at $p < 0.05$.

Results

No structural changes in the myocardium after 7 days cocaine administration via the tail vein. Cocaine has been reported to induce cardiovascular disorders in animal models via intraperitoneal administration. To assess the effect of cocaine on the myocardium in our model using tail vein administration, H&E and EMG staining of left ventricular specimens from the control group and cocaine group rats were conducted (Fig. 1). The myocardium of the cocaine group rats showed no signs of hypertrophy since the size and arrangement of myocardial fibers were retained after 20 mg/kg/day administration for 7 days. There was



◀ **Figure 2.** Maintained cardiac mitochondrial activity and elevated mitochondrial fission after cocaine administration. (A) Protein expressions of voltage-dependent anion-selective channel protein 2 (VDAC2), translocase of outer mitochondrial membrane 20 (TOM20), and mitochondria oxidative phosphorylation subunits (Oxphos) in rat left ventricle after cocaine administration. Levels of actin were served as an internal control. (B) Detection of endogenous Cox I activity in cardiac mitochondria isolated from myocardium samples from control and cocaine high dose group rats. (C) Transmission electron micrographs of left ventricular samples from control and cocaine group rats. Magnification, $\times 10,000$. White arrows indicate mitochondria. (D) The number of mitochondria per field in control and cocaine group rats. Each bar represents the mean and S.D. of 10 areas. (E) The area of mitochondria in control and cocaine group rats. Comparison of the distribution of mitochondrial area in control and cocaine group rats is shown. Over 100 mitochondria were measured in each group and the area was measured in cross-sectional views of cardiac myofibrils. (F) Dynamin-related protein 1 (Drp1), mitochondrial fission 1 protein (Fis1), Mitofusin 2 (Mfn2), and Optic atrophy type 1 (Opa1) expressions after cocaine administration as examined by qPCR. GAPDH levels served as an endogenous control. Each bar represents mean and S.D. * $p < 0.05$, ** $p < 0.01$, *** $p < 0.001$, *C I-V* complex I–V. *Con* control group, *Coc (L)* cocaine low dose group, *Coc (H)* cocaine high dose group, *RQ* relative quantification.

also no observable inflammatory infiltration or fibrosis deposition in the myocardium in the cocaine group. No significant pathological changes other than congestion were observed in the microphotographs of the cocaine high dose group. As a result, the histological findings suggest a basically normal myocardium after cocaine administration via the tail vein.

Unimpaired cardiac mitochondrial activity and elevated mitochondrial fission after 7 days cocaine administration via tail vein.

Next, we determined the effect of cocaine on cardiac mitochondrial status and function. Immunoblotting of mitochondria oxidative phosphorylation subunit proteins showed an increase in the complex I protein. Apart from complex I and IV proteins, the expressions of complex II, complex III, complex V, VDAC2, and TOM20 showed no significant changes after cocaine administration (Fig. 2A). To obtain a better understanding of cardiac mitochondrial function after cocaine administration, endogenous complex I activity assays using left ventricle samples from the control and cocaine high dose groups were conducted. Consistent with the immunoblotting result, the complex I activity of the cocaine high dose group myocardium was significantly elevated compared to the activity of the control group (Fig. 2B).

Owing to the seemingly normal mitochondrial status and function, transmission electron microscopy was conducted to acquire a direct observation of cardiac mitochondrial morphological changes after cocaine administration. As shown in Fig. 2C, the number of cardiac mitochondria was notably increased in the cocaine high dose group as compared to the control group (Fig. 2D). At the same time, the cross-sectional area of the cardiac mitochondria as checked on cross-sections of the myocardium decreased remarkably after cocaine administration (Fig. 2E).

Given the indications that the mitochondrial activity as well as homeostasis of the cardiomyocytes was maintained with the increased number of mitochondria, we suspect the cardiac mitochondrial dynamics were affected by cocaine administration. To examine this possibility, the relative levels of transcripts that participate in mitochondrial dynamics were evaluated by qPCR. Expression of the mitochondrial fission-related gene *Fis1* showed an apparent increase, while the expressions of mitochondrial fusion-related genes *Mfn2* and *Opa1* showed significant decreases in response to cocaine administration (Fig. 2F). These findings indicate that activated mitochondrial fission might be involved in the maintenance of mitochondrial activity as well as cardiac homeostasis.

Activation of mitochondrial biogenesis and nuclear translocation of PPAR α after 7 days cocaine administration via tail vein.

Mitochondrial biogenesis was another suspected participator in the maintenance of mitochondrial activity. We therefore examined the expressions of proteins related to cardiac mitochondrial biogenesis by immunoblotting. The expression of TFAM in the cocaine high dose group, was significantly increased as compared to its expression in the control group, whereas the expressions of PGC-1 and NRF1 showed no significant changes after cocaine administration (Fig. 3A). These findings indicate activated biogenesis and the likely activation of the NRF1-TFAM axis. Consequently, we examined PPAR α , an effector of PGC-1, by immunoblotting and immunohistochemistry. Although immunoblot analysis showed no significant change in PPAR α expression in the high dose cocaine group as compared to the control group (Fig. 3B), an apparent nuclear translocation of PPAR α after cocaine administration was observed by immunohistochemistry (Fig. 3C). These observations suggest the activation of mitochondrial biogenesis and the recruitment of PPAR α after cocaine administration.

Activation of cardiac mitochondrial unfolded protein response after 7 days cocaine administration via tail vein.

Finally, to clarify the role of UPR^{mt} in our observed effects of cocaine on cardiac mitochondria, UPR^{mt}-related regulators and factors were examined by qPCR, immunoblotting, and immunohistochemistry. The expressions of the major regulator of UPR^{mt} activation gene *ATF5*, transcription factor gene *CHOP*, and mitochondrial chaperone gene *HSP60* were all remarkably increased; however, the genes for other factors such as *LONP1*, *CLPP*, *mtDnaJ*, and *HSP10* were rather decreased (Fig. 4A). Further immunoblotting of ATF5 and CHOP revealed the same increase in ATF5 expression (Fig. 4B). The immunohistochemistry of ATF5 further revealed the nuclear translocation of ATF5 in cardiomyocytes after cocaine administration (Fig. 4C), consistent with the report that ATF5, once activated, undergoes nuclear translocation to signal UPR^{mt}⁴². These

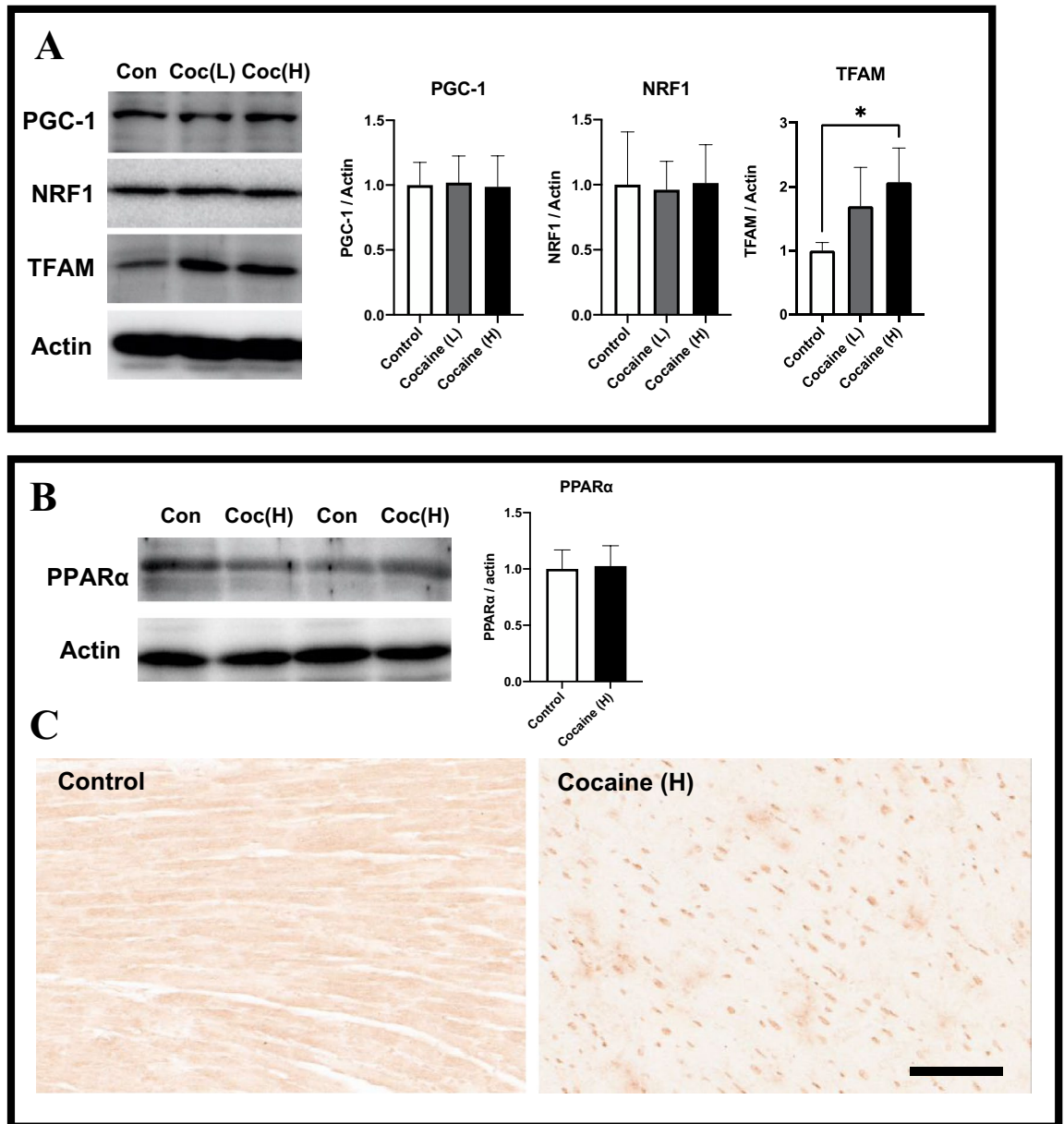


Figure 3. Activation of TFAM and nuclear translocation of PPAR α after cocaine administration. **(A)** Expressions of peroxisome proliferator-activated receptor-gamma coactivator 1 (PGC1), nuclear respiratory factor 1 (NRF1), and mitochondrial transcription factor A (TFAM) in rat left ventricle after cocaine administration. **(B)** Expression of peroxisome proliferator-activated receptor α (PPAR α) in rat left ventricle after cocaine administration. Actin levels served as an internal control. Each bar represents mean and S.D. * $p < 0.05$. **(C)** Immunohistochemistry of PPAR α in rat left ventricular samples from control and cocaine high dose groups showed apparent nuclear translocation of positive staining after cocaine administration. Scale bar = 100 μ m.

findings indicate the occurrence of cardiac UPR^{mt} after 7 days cocaine administration via tail vein, although it seems that UPR^{mt} occurred in an incomplete or atypical manner as compared with typical UPR^{mt}.

Discussion

Abundant evidence implicates cocaine abuse in cardiovascular disease. The clinical short-term consequences of cocaine intoxication include acute myocardial infarction¹⁰, arterial wall inflammation⁴⁷, endocarditis⁴⁸, interstitial inflammatory infiltration, and fibrosis⁴⁹. Animal cocaine models in which cocaine is delivered by intraperitoneal injection also reproduce cardiomyopathies such as inflammatory infiltration⁵⁰, contraction band necrosis⁵¹, and left ventricular dysfunction¹³. Intriguingly, no observation of notable structural changes was found in rat myocardium after 7 days of cocaine administration (20 mg/kg/day) via tail vein in our experiments. This might be owing to the relatively short experimental period of our study. Additionally, although there are no comparative studies on toxicity of cocaine administered via different routes, one report has suggested a lower toxicity of

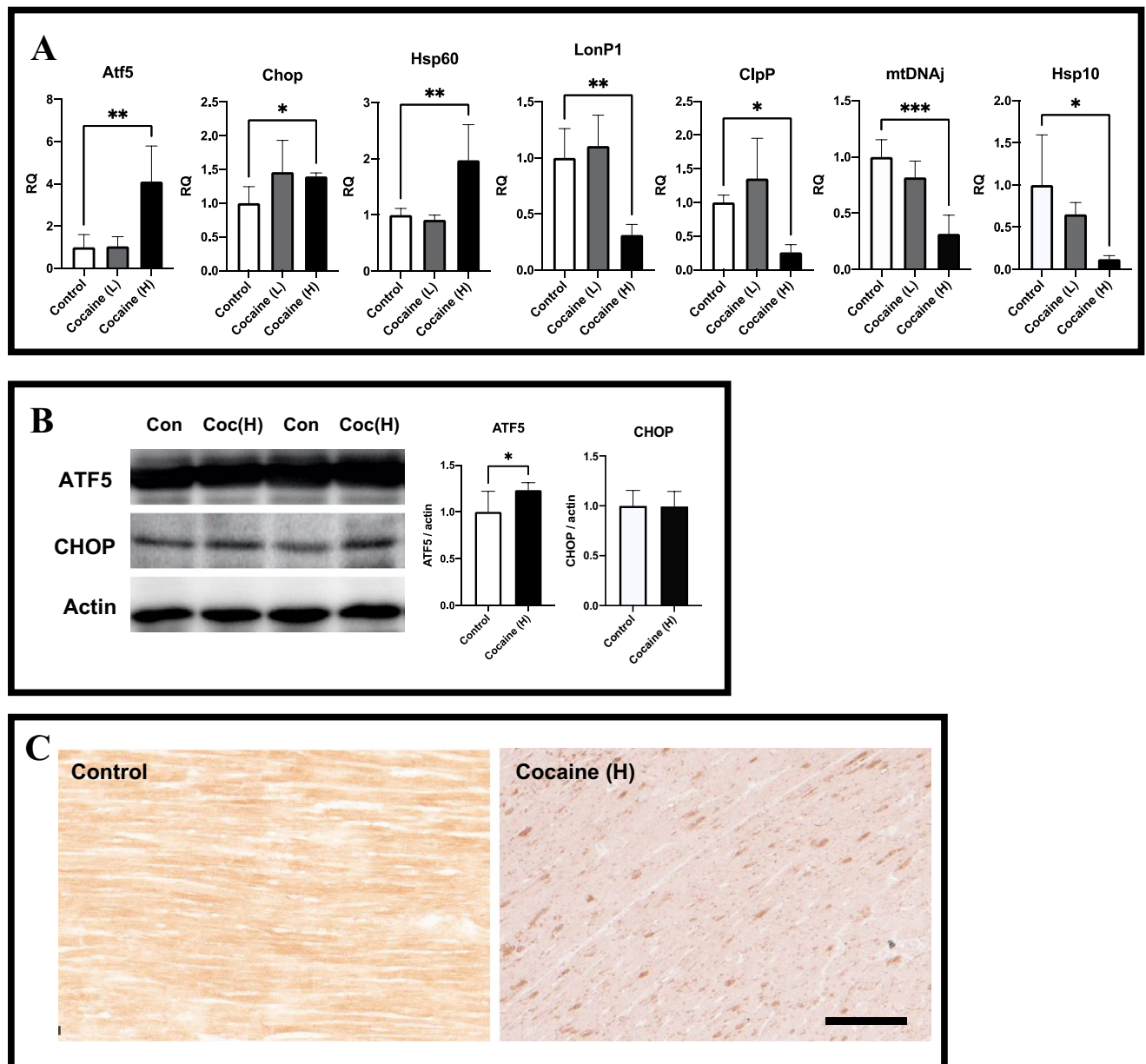


Figure 4. Partial activation of cardiac mitochondrial unfolded protein response after cocaine administration. **(A)** The expressions of activating transcription factor 5 (Atf5), CCAT-enhancer-binding protein homologous protein (CHOP), heat shock 60 kDa protein 1 (Hsp60), Lon protease homolog, mitochondrial (LonP1), ATP-dependent Clp protease proteolytic subunit (ClpP), mitochondrial pre-sequence translocase-associated motor complex protein (mtDNAj), and heat shock 10 kDa protein (Hsp10) after cocaine administration as examined by qPCR. GAPDH levels served as an endogenous control. RQ, relative quantification. **(B)** Expressions of ATF5 and CHOP in rat left ventricle after cocaine administration. Actin levels served as an internal control. Each bar represents mean and S.D. Coc (H), cocaine high dose group, * $p < 0.05$, ** $p < 0.01$, *** $p < 0.001$. **(C)** Immunohistochemistry of ATF5 in rat left ventricular samples from control and cocaine high dose groups showed an apparent nuclear translocation of positive staining after cocaine administration. cocaine (H), cocaine high dose group. Scale bar = 100 μ m.

gold nanoparticles administered via the tail vein as compared to intraperitoneal injection⁵². As a result, it is also possible that our negative histological findings of structural changes in myocardium were due to the influence of the different administration route of cocaine as compared with previous researches. We further investigated the status of cardiac mitochondria after cocaine administration because mitochondrial dysfunction is one of the hallmarks of cocaine cardiotoxicity. These examinations revealed normally reserved mitochondrial status and function. The function of complex I, the first and largest enzyme of ETC, and most of its core subunits, which are mitochondrially encoded proteins⁵³, were elevated rather than impaired after 7 days of cocaine administration via the tail vein. It has been repeatedly reported that cocaine-induced oxidative stress increases the production of ROS, damages the ETC, suppresses the generation of ATP⁵⁴, as well as compromises the antioxidative system^{50,54},

and all of these eventually results in cardiac mitochondrial dysfunction^{17,55}. Animal models of cocaine abuse have also revealed an extensively decreased expression of mitochondrial genes and proteins^{56,57}. The rare but meaningful findings in our study showed a still normally maintained mitochondrial status after cocaine administration, which suggests that a mitochondria-targeted self-compensation mechanism against cocaine cardiotoxicity was activated prior to the occurrence of any structural changes in myocardium.

As stated above, mechanisms such as mitochondrial dynamics, biogenesis, and UPR^{mt} help to preserve mitochondrial homeostasis in cardiomyocytes and act protectively against detrimental effects. In particular, mitochondrial dynamics and biogenesis take part in determining mitochondrial quality and abundance, thereby maintaining adequate myocardial function^{26,27,58–61}. Elevated mitochondrial fission and biogenesis meet the increased energy demand of cardiac myocytes under stress or ischemic injury or the harmful effects of chemicals^{26,58,62}. We discovered that it is the same circumstance in cardiac mitochondria after cocaine administration. In this study, we found the activations of mitochondrial fission and biogenesis, together with downregulated mitochondrial fusion gene expression. These effects may act together to profoundly increase the number of mitochondria, as we observed by electron microscopy, so as to maintain normal cardiac function under the detrimental effects of cocaine. Mitochondrial Fis1 recruitment has been demonstrated as an early event in the cardiac pathological process^{63,64}, and the elevated fission machinery ultimately results in cardiomyopathy^{20,26}. It is consistent with our view of the mitochondrial compensatory stage ahead of any pathological changes. In addition, during pathological cardiac remodeling, TFAM protects the mitochondrial DNA from mutation, and its overexpression is beneficial to the recovery of cardiac function⁶⁵. It is likely that this protective effect of TFAM might also participate in the specific upregulation of mitochondrial DNA and preserved function of complex I seen in this study. Meanwhile, as the effector of PGC-1, PPAR α also participates in mitochondrial biogenesis and homeostasis because of its central role in fatty acid oxidation and other lipid metabolism events^{66–68}. However, the involvement of PPAR α in the cardiotoxicity of cocaine has not been illustrated. Our immunohistochemical observation indicates the recruitment of PPAR α in the myocardium after cocaine administration. This might be related to our observation of elevated mitochondrial biogenesis in cocaine group rats and implies a potential role of PPAR α in resistance to the cardiotoxicity of cocaine. UPR^{mt} is another potential protective mechanism to explain the unimpaired mitochondrial function we observed. UPR^{mt} activation has been shown to be important for the normal function of cardiac myocytes⁴³. Among numerous involved factors, ATF5 should be involved in the UPR^{mt} cardioprotective effects against stress, cardiac dysfunction, and pathological remodeling, because its activation and nuclear translocation trigger the downstream responses of UPR^{mt}^{69,70}. CHOP and Hsp60, on the other hand, play key roles in maintaining mitochondrial homeostasis in UPR^{mt}⁷¹. Our examination of UPR^{mt} revealed an interesting phenomenon that instead of all UPR^{mt} factors being collectively upregulated after cocaine administration, the expressions of several UPR^{mt} factors decreased significantly. It has been reported that Lon regulates mitochondrial transcription by selectively degrading TFAM⁷², and the absence of *CLPP* reduces mitochondrial cardiomyopathy⁷³. These findings suggest that the downregulation of *LONP1* and *CLPP* that we observed might also play a protective role against cocaine cardiotoxicity. Nevertheless, further research will be required in order to fully understand the paradoxical expression of UPR^{mt} factors that we observed. So far, our findings indicate that UPR^{mt} participates in cardiac mitochondrial protection against the cardiotoxicity of cocaine, even if not complete and collectively activated at an early stage.

In conclusion, we demonstrated that 7-day 20 mg/kg/day cocaine administration to rats via the tail vein results in elevated cardiac mitochondrial fission and biogenesis, the recruitment of PPAR α , and the activation of mitochondrial protecting UPR^{mt} in the myocardium. The limit of this study is the insufficient data of cardiac and mitochondrial functional changes, as well as stress accumulation after cocaine administration, which necessitates more functional assessments of heart and mitochondria in following studies, such as echocardiography, respiration profiles, and ATP production rates. It is worth noticing that the differences might present among individual models, but our findings should be beneficial for an advanced understanding of the cardiotoxicity of cocaine, especially the early events following cocaine exposure.

Received: 19 September 2021; Accepted: 30 November 2021

Published online: 16 December 2021

References

- Karila, L. *et al.* Cocaine addiction: Current data for the clinician. *Presse Med.* **43**, 9–17. <https://doi.org/10.1016/j.lpm.2013.01.069> (2014).
- Lange, R. A. *et al.* Cocaine-induced coronary-artery vasoconstriction. *N. Engl. J. Med.* **321**, 1557–1562. <https://doi.org/10.1056/NEJM198912073212301> (1989).
- Vongpatanasin, W., Mansour, Y., Chavoshan, B., Arbiq, D. & Victor, R. G. Cocaine stimulates the human cardiovascular system via a central mechanism of action. *Circulation* **100**, 497–502. <https://doi.org/10.1161/01.cir.100.5.497> (1999).
- Lange, R. A. & Hillis, L. D. Cardiovascular complications of cocaine use. *N. Engl. J. Med.* **345**, 351–358. <https://doi.org/10.1056/NEJM200108023450507> (2001).
- Resnick, R. B., Kestenbaum, R. S. & Schwartz, L. K. Acute systemic effects of cocaine in man: A controlled study by intranasal and intravenous routes. *Science* **195**, 696–698. <https://doi.org/10.1126/science.841307> (1977).
- Brickner, M. E., Willard, J. E., Eichhorn, E. J., Black, J. & Grayburn, P. A. Left ventricular hypertrophy associated with chronic cocaine abuse. *Circulation* **84**, 1130–1135. <https://doi.org/10.1161/01.cir.84.3.1130> (1991).
- Pitts, W. R., Lange, R. A., Cigarroa, J. E. & Hillis, L. D. Cocaine-induced myocardial ischemia and infarction: Pathophysiology, recognition, and management. *Prog. Cardiovasc. Dis.* **40**, 65–76. [https://doi.org/10.1016/s0033-0620\(97\)80023-0](https://doi.org/10.1016/s0033-0620(97)80023-0) (1997).
- Mittleman, M. A. *et al.* Triggering of myocardial infarction by cocaine. *Circulation* **99**, 2737–2741. <https://doi.org/10.1161/01.cir.99.21.2737> (1999).
- Kloner, R. A., Hale, S., Alker, K. & Rezkalla, S. The effects of acute and chronic cocaine use on the heart. *Circulation* **85**, 407–419. <https://doi.org/10.1161/01.cir.85.2.407> (1992).

10. Schwartz, B. G., Rezkalla, S. & Kloner, R. A. Cardiovascular effects of cocaine. *Circulation* **122**, 2558–2569. <https://doi.org/10.1161/CIRCULATIONAHA.110.940569> (2010).
11. Billman, G. E. Mechanisms responsible for the cardiotoxic effects of cocaine. *FASEB J.* **4**, 2469–2475. <https://doi.org/10.1096/fasebj.4.8.2185973> (1990).
12. Beckman, K. J. *et al.* Hemodynamic and electrophysiological actions of cocaine. Effects of sodium bicarbonate as an antidote in dogs. *Circulation* **83**, 1799–1807. <https://doi.org/10.1161/01.cir.83.5.1799> (1991).
13. Moritz, F. *et al.* Role of reactive oxygen species in cocaine-induced cardiac dysfunction. *Cardiovasc. Res.* **59**, 834–843. [https://doi.org/10.1016/s0008-6363\(03\)00499-1](https://doi.org/10.1016/s0008-6363(03)00499-1) (2003).
14. Moritz, F. *et al.* Selenium diet-supplementation improves cocaine-induced myocardial oxidative stress and prevents cardiac dysfunction in rats. *Fundam. Clin. Pharmacol.* **18**, 431–436. <https://doi.org/10.1111/j.1472-8206.2004.00255.x> (2004).
15. Isabelle, M. *et al.* NADPH oxidase inhibition prevents cocaine-induced up-regulation of xanthine oxidoreductase and cardiac dysfunction. *J. Mol. Cell Cardiol.* **42**, 326–332. <https://doi.org/10.1016/j.yjmcc.2006.11.011> (2007).
16. Vergeade, A. *et al.* Mitochondrial impairment contributes to cocaine-induced cardiac dysfunction: Prevention by the targeted antioxidant MitoQ. *Free Radic. Biol. Med.* **49**, 748–756. <https://doi.org/10.1016/j.freeradbiomed.2010.05.024> (2010).
17. Cerretani, D. *et al.* Role of oxidative stress in cocaine-induced cardiotoxicity and cocaine-related death. *Curr. Med. Chem.* **19**, 5619–5623. <https://doi.org/10.2174/092986712803988785> (2012).
18. Marin-Garcia, J., Goldenthal, M. J. & Moe, G. W. Mitochondrial pathology in cardiac failure. *Cardiovasc. Res.* **49**, 17–26. [https://doi.org/10.1016/s0008-6363\(00\)00241-8](https://doi.org/10.1016/s0008-6363(00)00241-8) (2001).
19. Hall, A. R., Burke, N., Dongworth, R. K. & Hausenloy, D. J. Mitochondrial fusion and fission proteins: Novel therapeutic targets for combating cardiovascular disease. *Br. J. Pharmacol.* **171**, 1890–1906. <https://doi.org/10.1111/bph.12516> (2014).
20. Marin-Garcia, J. & Akhmedov, A. T. Mitochondrial dynamics and cell death in heart failure. *Heart Fail. Rev.* **21**, 123–136. <https://doi.org/10.1007/s10741-016-9530-2> (2016).
21. Pellegrini, L. & Scorrano, L. A cut short to death: Parl and Opa1 in the regulation of mitochondrial morphology and apoptosis. *Cell Death Differ.* **14**, 1275–1284. <https://doi.org/10.1038/sj.cdd.4402145> (2007).
22. Hausenloy, D. J. & Ruiz-Meana, M. Not just the powerhouse of the cell: Emerging roles for mitochondria in the heart. *Cardiovasc. Res.* **88**, 5–6. <https://doi.org/10.1093/cvr/cvq259> (2010).
23. Nunnari, J. & Suomalainen, A. Mitochondria: In sickness and in health. *Cell* **148**, 1145–1159. <https://doi.org/10.1016/j.cell.2012.02.035> (2012).
24. Brown, D. A. & O'Rourke, B. Cardiac mitochondria and arrhythmias. *Cardiovasc. Res.* **88**, 241–249. <https://doi.org/10.1093/cvr/cvq231> (2010).
25. Rosca, M. G. & Hoppel, C. L. Mitochondria in heart failure. *Cardiovasc. Res.* **88**, 40–50. <https://doi.org/10.1093/cvr/cvq240> (2010).
26. Vasquez-Trincado, C. *et al.* Mitochondrial dynamics, mitophagy and cardiovascular disease. *J. Physiol.* **594**, 509–525. <https://doi.org/10.1113/jp271301> (2016).
27. Westermann, B. Mitochondrial fusion and fission in cell life and death. *Nat. Rev. Mol. Cell Biol.* **11**, 872–884. <https://doi.org/10.1038/nrm3013> (2010).
28. Friedman, J. R. & Nunnari, J. Mitochondrial form and function. *Nature* **505**, 335–343. <https://doi.org/10.1038/nature12985> (2014).
29. Alexander, C. *et al.* OPA1, encoding a dynamin-related GTPase, is mutated in autosomal dominant optic atrophy linked to chromosome 3q28. *Nat. Genet.* **26**, 211–215. <https://doi.org/10.1038/79944> (2000).
30. Ferguson, S. M. & De Camilli, P. Dynamin, a membrane-remodelling GTPase. *Nat. Rev. Mol. Cell Biol.* **13**, 75–88. <https://doi.org/10.1038/nrm3266> (2012).
31. Sprenger, H. G. & Langer, T. The good and the bad of mitochondrial breakups. *Trends Cell Biol.* **29**, 888–900. <https://doi.org/10.1016/j.tcb.2019.08.003> (2019).
32. Lehman, J. J. *et al.* Peroxisome proliferator-activated receptor gamma coactivator-1 promotes cardiac mitochondrial biogenesis. *J. Clin. Investig.* **106**, 847–856. <https://doi.org/10.1172/JCI10268> (2000).
33. Dorn, G. W. 2nd., Vega, R. B. & Kelly, D. P. Mitochondrial biogenesis and dynamics in the developing and diseased heart. *Genes Dev.* **29**, 1981–1991. <https://doi.org/10.1101/gad.269894.115> (2015).
34. Liesa, M., Palacin, M. & Zorzano, A. Mitochondrial dynamics in mammalian health and disease. *Physiol. Rev.* **89**, 799–845. <https://doi.org/10.1152/physrev.00030.2008> (2009).
35. Youle, R. J. & van der Bliek, A. M. Mitochondrial fission, fusion, and stress. *Science* **337**, 1062–1065. <https://doi.org/10.1126/science.1219855> (2012).
36. Ong, S. B., Hall, A. R. & Hausenloy, D. J. Mitochondrial dynamics in cardiovascular health and disease. *Antioxid. Redox Signal* **19**, 400–414. <https://doi.org/10.1089/ars.2012.4777> (2013).
37. Dorn, G. W. Mitochondrial dynamism and heart disease: Changing shape and shaping change. *EMBO Mol. Med.* **7**, 865–877. <https://doi.org/10.15252/emmm.201404575> (2015).
38. Sharp, W. W. & Archer, S. L. Mitochondrial dynamics in cardiovascular disease: Fission and fusion foretell form and function. *J. Mol. Med. (Berl.)* **93**, 225–228. <https://doi.org/10.1007/s00109-015-1258-2> (2015).
39. Nargund, A. M., Fiorese, C. J., Pellegrino, M. W., Deng, P. & Haynes, C. M. Mitochondrial and nuclear accumulation of the transcription factor ATFS-1 promotes OXPHOS recovery during the UPR(mt). *Mol. Cell* **58**, 123–133. <https://doi.org/10.1016/j.molcel.2015.02.008> (2015).
40. Nargund, A. M., Pellegrino, M. W., Fiorese, C. J., Baker, B. M. & Haynes, C. M. Mitochondrial import efficiency of ATFS-1 regulates mitochondrial UPR activation. *Science* **337**, 587–590. <https://doi.org/10.1126/science.1223560> (2012).
41. Shpilka, T. & Haynes, C. M. The mitochondrial UPR: Mechanisms, physiological functions and implications in ageing. *Nat. Rev. Mol. Cell Biol.* **19**, 109–120. <https://doi.org/10.1038/nrm.2017.110> (2018).
42. Fiorese, C. J. *et al.* The transcription factor ATF5 mediates a mammalian mitochondrial UPR. *Curr. Biol.* **26**, 2037–2043. <https://doi.org/10.1016/j.cub.2016.06.002> (2016).
43. Quiles, J. M. & Gustafsson, A. B. Mitochondrial quality control and cellular proteostasis: Two sides of the same coin. *Front. Physiol.* **11**, 515. <https://doi.org/10.3389/fphys.2020.00515> (2020).
44. Heard, K., Palmer, R. & Zahniser, N. R. Mechanisms of acute cocaine toxicity. *Open Pharmacol. J.* **2**, 70–78. <https://doi.org/10.2174/1874143600802010070> (2008).
45. Nair, A. B. & Jacob, S. A simple practice guide for dose conversion between animals and human. *J. Basic Clin. Pharm.* **7**, 27–31. <https://doi.org/10.4103/0976-0105.177703> (2016).
46. Funakoshi, T., Furukawa, M., Aki, T. & Uemura, K. Repeated exposure of cocaine alters mitochondrial dynamics in mouse neuroblastoma Neuro2a. *Neurotoxicology* **75**, 70–77. <https://doi.org/10.1016/j.neuro.2019.09.001> (2019).
47. Kolodgie, F. D., Virmani, R., Cornhill, J. F., Herderick, E. E. & Smialek, J. Increase in atherosclerosis and adventitial mast cells in cocaine abusers: An alternative mechanism of cocaine-associated coronary vasospasm and thrombosis. *J. Am. Coll. Cardiol.* **17**, 1553–1560. [https://doi.org/10.1016/0735-1097\(91\)90646-q](https://doi.org/10.1016/0735-1097(91)90646-q) (1991).
48. Chambers, H. F., Morris, D. L., Tauber, M. G. & Modin, G. Cocaine use and the risk for endocarditis in intravenous drug users. *Ann. Intern. Med.* **106**, 833–836. <https://doi.org/10.7326/0003-4819-106-6-833> (1987).
49. Tazelaar, H. D., Karch, S. B., Stephens, B. G. & Billingham, M. E. Cocaine and the heart. *Hum. Pathol.* **18**, 195–199. [https://doi.org/10.1016/s0046-8177\(87\)80338-6](https://doi.org/10.1016/s0046-8177(87)80338-6) (1987).

50. Devi, B. G. & Chan, A. W. Effect of cocaine on cardiac biochemical functions. *J. Cardiovasc. Pharmacol.* **33**, 1–6. <https://doi.org/10.1097/00005344-199901000-00001> (1999).
51. Fineschi, V. *et al.* Markers of cardiac oxidative stress and altered morphology after intraperitoneal cocaine injection in a rat model. *Int. J. Legal Med.* **114**, 323–330. <https://doi.org/10.1007/s004140000194> (2001).
52. Zhang, X. D. *et al.* Toxicologic effects of gold nanoparticles in vivo by different administration routes. *Int. J. Nanomed.* **5**, 771–781. <https://doi.org/10.2147/IJN.S8428> (2010).
53. Brandt, U. Energy converting NADH:quinone oxidoreductase (complex I). *Annu. Rev. Biochem.* **75**, 69–92. <https://doi.org/10.1146/annurev.biochem.75.103004.142539> (2006).
54. Boess, F., Ndikum-Moffor, F. M., Boelsterli, U. A. & Roberts, S. M. Effects of cocaine and its oxidative metabolites on mitochondrial respiration and generation of reactive oxygen species. *Biochem. Pharmacol.* **60**, 615–623. [https://doi.org/10.1016/s0006-2952\(00\)00355-5](https://doi.org/10.1016/s0006-2952(00)00355-5) (2000).
55. Liaudet, L., Calderari, B. & Pacher, P. Pathophysiological mechanisms of catecholamine and cocaine-mediated cardiotoxicity. *Heart Fail. Rev.* **19**, 815–824. <https://doi.org/10.1007/s10741-014-9418-y> (2014).
56. Yuferov, V. *et al.* Differential gene expression in the rat caudate putamen after “binge” cocaine administration: Advantage of triplicate microarray analysis. *Synapse* **48**, 157–169. <https://doi.org/10.1002/syn.10198> (2003).
57. Dietrich, J. B., Poirier, R., Aunis, D. & Zwiller, J. Cocaine downregulates the expression of the mitochondrial genome in rat brain. *Ann. N. Y. Acad. Sci.* **1025**, 345–350. <https://doi.org/10.1196/annals.1316.042> (2004).
58. Huss, J. M. & Kelly, D. P. Mitochondrial energy metabolism in heart failure: A question of balance. *J. Clin. Investig.* **115**, 547–555. <https://doi.org/10.1172/JCI24405> (2005).
59. Pich, S. *et al.* The Charcot-Marie-Tooth type 2A gene product, Mfn2, up-regulates fuel oxidation through expression of OXPHOS system. *Hum. Mol. Genet.* **14**, 1405–1415. <https://doi.org/10.1093/hmg/ddi149> (2005).
60. Zorzano, A., Liesa, M. & Palacin, M. Role of mitochondrial dynamics proteins in the pathophysiology of obesity and type 2 diabetes. *Int. J. Biochem. Cell Biol.* **41**, 1846–1854. <https://doi.org/10.1016/j.biocel.2009.02.004> (2009).
61. Chen, Y. & Dorn, G. W. PINK1-phosphorylated mitofusin 2 is a Parkin receptor for culling damaged mitochondria. *Science* **340**, 471–475. <https://doi.org/10.1126/science.1231031> (2013).
62. Brady, N. R., Hamacher-Brady, A. & Gottlieb, R. A. Proapoptotic BCL-2 family members and mitochondrial dysfunction during ischemia/reperfusion injury, a study employing cardiac HL-1 cells and GFP biosensors. *Biochim. Biophys. Acta* **1757**, 667–678. <https://doi.org/10.1016/j.bbabi.2006.04.011> (2006).
63. Twig, G. *et al.* Fission and selective fusion govern mitochondrial segregation and elimination by autophagy. *EMBO J.* **27**, 433–446. <https://doi.org/10.1038/sj.emboj.7601963> (2008).
64. Lee, Y., Lee, H. Y., Hanna, R. A. & Gustafsson, A. B. Mitochondrial autophagy by Bnip3 involves Drp1-mediated mitochondrial fission and recruitment of Parkin in cardiac myocytes. *Am. J. Physiol. Heart Circ. Physiol.* **301**, H1924–H1931. <https://doi.org/10.1152/ajpheart.00368.2011> (2011).
65. Kunkel, G. H., Kunkel, C. J., Ozuna, H., Miralda, I. & Tyagi, S. C. TFAM overexpression reduces pathological cardiac remodeling. *Mol. Cell Biochem.* **454**, 139–152. <https://doi.org/10.1007/s11010-018-3459-9> (2019).
66. Brandt, J. M., Djouadi, F. & Kelly, D. P. Fatty acids activate transcription of the muscle carnitine palmitoyltransferase I gene in cardiac myocytes via the peroxisome proliferator-activated receptor alpha. *J. Biol. Chem.* **273**, 23786–23792. <https://doi.org/10.1074/jbc.273.37.23786> (1998).
67. Aoyama, T. *et al.* Altered constitutive expression of fatty acid-metabolizing enzymes in mice lacking the peroxisome proliferator-activated receptor alpha (PPARalpha). *J. Biol. Chem.* **273**, 5678–5684. <https://doi.org/10.1074/jbc.273.10.5678> (1998).
68. Djouadi, F. *et al.* The role of the peroxisome proliferator-activated receptor alpha (PPAR alpha) in the control of cardiac lipid metabolism. *Prostagland. Leukot. Essent Fatty Acids* **60**, 339–343. [https://doi.org/10.1016/s0952-3278\(99\)80009-x](https://doi.org/10.1016/s0952-3278(99)80009-x) (1999).
69. Smyrniak, I. *et al.* Cardioprotective effect of the mitochondrial unfolded protein response during chronic pressure overload. *J. Am. Coll. Cardiol.* **73**, 1795–1806. <https://doi.org/10.1016/j.jacc.2018.12.087> (2019).
70. Wang, Y. T. *et al.* Cardioprotection by the mitochondrial unfolded protein response requires ATF5. *Am. J. Physiol. Heart Circ. Physiol.* **317**, H472–H478. <https://doi.org/10.1152/ajpheart.00244.2019> (2019).
71. Zhao, Q. *et al.* A mitochondrial specific stress response in mammalian cells. *EMBO J.* **21**, 4411–4419. <https://doi.org/10.1093/emboj/cdf445> (2002).
72. Matsushima, Y., Goto, Y. & Kaguni, L. S. Mitochondrial Lon protease regulates mitochondrial DNA copy number and transcription by selective degradation of mitochondrial transcription factor A (TFAM). *Proc. Natl. Acad. Sci. U.S.A.* **107**, 18410–18415. <https://doi.org/10.1073/pnas.1008924107> (2010).
73. Seiferling, D. *et al.* Loss of CLPP alleviates mitochondrial cardiomyopathy without affecting the mammalian UPRmt. *EMBO Rep.* **17**, 953–964. <https://doi.org/10.15252/embr.201642077> (2016).

Author contributions

S.W., Ka.U. and T.A. designed the experiments and S.W. performed most of the experiments. S.W. and T.A. wrote the manuscript. T.F. performed EM analysis and edited the manuscript. Ka.U. and Ko.U. interpreted the results and edited the manuscript. All authors reviewed and approved the manuscript.

Funding

The funding was provided by Ministry of Education, Culture, Sports, Science and Technology (19K10680, 18K19670).

Competing interests

One of the authors (S.W.) receives a scholarship funded by the Cooperation Program between Tokyo Medical and Dental University (TMDU), Sony Corporation and Sony Group Corporation. Other authors declare no competing interests.

Additional information

Supplementary Information The online version contains supplementary material available at <https://doi.org/10.1038/s41598-021-03631-y>.

Correspondence and requests for materials should be addressed to T.A.

Reprints and permissions information is available at www.nature.com/reprints.

Publisher's note Springer Nature remains neutral with regard to jurisdictional claims in published maps and institutional affiliations.



Open Access This article is licensed under a Creative Commons Attribution 4.0 International License, which permits use, sharing, adaptation, distribution and reproduction in any medium or format, as long as you give appropriate credit to the original author(s) and the source, provide a link to the Creative Commons licence, and indicate if changes were made. The images or other third party material in this article are included in the article's Creative Commons licence, unless indicated otherwise in a credit line to the material. If material is not included in the article's Creative Commons licence and your intended use is not permitted by statutory regulation or exceeds the permitted use, you will need to obtain permission directly from the copyright holder. To view a copy of this licence, visit <http://creativecommons.org/licenses/by/4.0/>.

© The Author(s) 2021